Scientific Research Publishing

**Energy and Power Engineering, 2017, 9, 309-323**
http://www.scirp.org/journal/epe
ISSN Online: 1947-3818
ISSN Print: 1949-243X

# Improving the Performance of Photovoltaic Power Plants with Determinative Module for the Cooling System

**Vinícius O. da Silva*, Miguel E. M. Udaeta, André L. V. Gimenes, Angélica L. Linhares**

Department of Energy and Electrical Automation Engineering of the Polytechnic School, University of São Paulo Affiliation, São Paulo, Brazil

Email: *vinicius.oliveira.silva@usp.br

**How to cite this paper:** da Silva, V.O., Udaeta, M.E.M., Gimenes, A.L.V. and Linhares, A.L. (2017) Improving the Performance of Photovoltaic Power Plants with Determinative Module for the Cooling System. *Energy and Power Engineering*, **9**, 309-323.
https://doi.org/10.4236/epe.2017.95021

**Received:** April 2, 2017
**Accepted:** May 28, 2017
**Published:** May 31, 2017



## Abstract

The objective of this work is to analyze and evaluate the impact of cooling systems on photovoltaic modules (for electricity generation), applied at a pilot Testing Facility. The results obtained during this step are used as input in order to determine the best model to be applied at a real-scale Photovoltaic Power Plant (PVPP). This methodology is based on the monitoring and supervision of the operating temperature of commercial photovoltaic modules (PV), both with and without cooling systems, as well as on the study of the water supply design of the cooling system applied on a micro photovoltaic power plant which is connected to the commercial network. Through the analysis of the data, we observed that photovoltaic modules with cooling systems always operate at lower temperatures than the ones without cooling systems. During the testing period, the operating temperatures of the photovoltaic modules without cooling systems were above 60˚C (with a maximum temperature equaling 68.06˚C), whereas the maximum temperatures registered on the sensors of the model "A" were 43.55˚C and 44.75˚C, and the ones registered on the sensors of the model "B" were 46.76 and 48.33˚C. Therefore, we conclude that the photovoltaic module with the cooling system model "A" is the most suitable for large-scale application, since it was the only model to present temperatures lower than the nominal operating condition temperature (NOCT) of the cell (47˚C ± 2˚C).

## Keywords

Solar Energy, Photovoltaic/Thermal, Cooling Photovoltaic System, Thermal Performance

## 1. Introduction

Research and Development (R & D) entail a methodology and/or a scientific method which provides the guidelines for reaching a certain goal. Moreover, it entails an infinite number of tests, reproductions, and validations, guaranteeing the validity of the research. The empirical method, which is based on experiment and observation, generates knowledge that enables the evaluation of specific phenomena, providing a solid basis for the process of decision-making. Therefore, it is a tool that enables the observer to conclude his experiment and/or theory based on facts [1].

The Testing Facility (TF) (see **Figure 1**) used for the selection of the final model of the Modular Cooling Unit (MCU) presents the same constructive characteristics with the Photovoltaic Power Plant (PVPP) [2]. The TF is a micro PVPP containing 5 rigid p-Si PV modules, with the total dimensions of 1.976 × 990 × 50 mm, its total weight equals 23 kg and has a power of 290 WP in each one of the modules [3], accounting for a total power of 1450 WP. The modules are arranged in a series and are connected to a grid-tie inverter which converts the output electricity from a direct current (DC) into an alternating current (AC) at 220 V. This guarantees the security of the TF, and stores the data of the electricity generation.

In terms of physical architecture, the TF has a metallic structure to support the modules which consist of zinc-coated steel beams connected to two horizontal concrete columns on the building terrace. Furthermore, the metallic beams present several holes along their length where a power box is installed in order to regulate the energy input of the water pumps [4] which are responsible for the water supply of the cooling systems. Additionally, a data logger, which is responsible for the storage of the data measured by the temperature sensors and registers the operating temperatures of the PV modules (both with and without a cooling system), is also installed.

**Figure 1.** Test uniti (TF).

Thus, the aim of this work is to systematically study and analyze the performance of the models of Modular Cooling Units (MCU) applied at an on-grid micro PVPP in order to select the model with the best thermal performance.

This methodology is based on a detailed description of the procedures and empirical methods applied on the operational tests used at the testing facility (TF) which was designed as a model for the monitoring and supervision of such procedures.

## 2. Cooling System of the TF

Since the following are subject to weather conditions, the operational tests on the TF's comprise of measurements of temperature, energy production, and water-use; evaluation of the process of installation of the cooling system, and the resistance and lifetime of the materials during the operation. The operation of the cooling system is described in Figure 2.

- At point 1, supply line. The water circulates permanently in order to reduce the operating temperature on the PV modules. This line is filled by two reservoirs of 10.0 $m^3$ each, providing water to the MCU, which are connected in a series;
- Point 2, discharge line, conducts the cooling fluid from the exit of the cooling system to the reservoir. Thus, all the water used in the system is returned to the reservoir, avoiding extra costs regarding water withdraws;
- The module PV-2, PVa (with cooling system), receives the model B of the MCU;
- The module PV-3 receives the model A of the MCU;
- The module PV-5 receives no MCU and is used for comparison purposes.

### 2.1. Temperature Control and Monitoring System of the TF

The system that measures the temperatures consists of six thermal resistances,

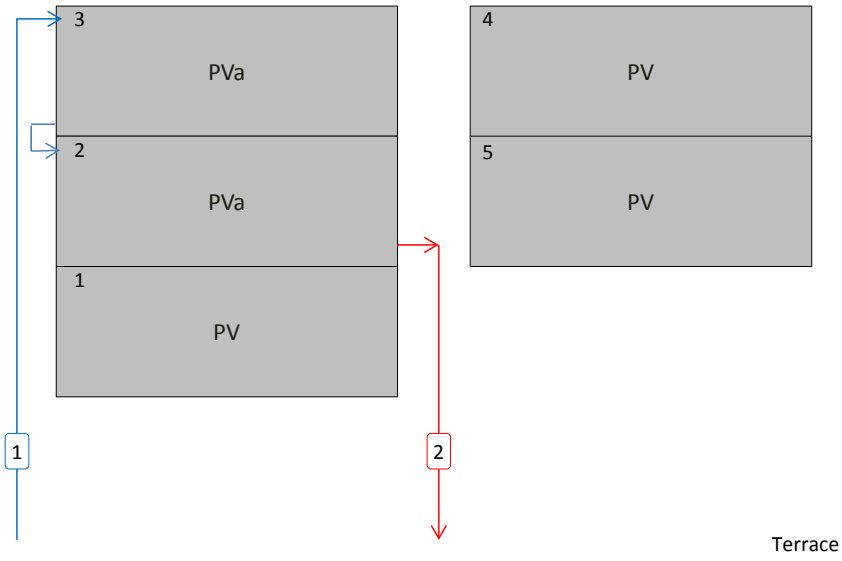


Figure 2. Scheme of the cooling system of the modules of the TF.

type PT-100 [5], with an output signal compatible to the datalogger [6], and a thermographic camera [7]. The configuration of the PT-100 sensors is identical on all the PV modules (see **Figure 3**). For each module, a sensor is applied at the center, Sensor Middle ("Meio") or SM, another one is applied near the junction box, called Sensor Point ("Ponta") or SP (see **Table 1**), directly applied at the inferior surface of the PV module. The PV modules which are coupled with cooling systems present two holes on the metallic sheet of the absorber, in order to permit the direct contact between the sensor and the inferior surface of the PV module. The thermographic camera measures and verifies the distribution of the temperature on the PV modules and on the MCU, operating at pre-determined times, 10:00 am, 12:00 pm, and 03:00 pm.

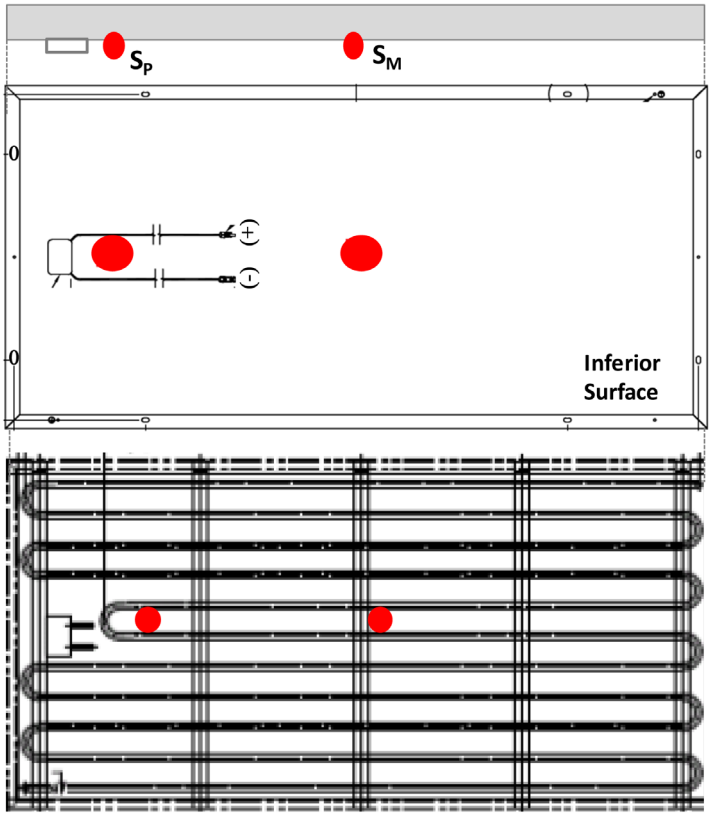


**Figure 3.** Position of the PT-100 sensors on the PV modules.

**Table 1.** Identification and position of the MCU models and temperature sensors.

| PV | Code PV | Cooling Model | Sensor PT-100 | Code PT-100 |
|---|---|---|---|---|
| 1 | PV | - | - | - |
| 2 | PVa | Model B (140.0 mm) | SM<br>SP | Meio_B<br>Ponta_B |
| 3 | PVa | Model A (85.0 mm) | SM<br>SP | Meio_A<br>Ponta_A |
| 4 | PV | - | - | - |
| 5 | PV | - | SM<br>SP | Meio_Sem<br>Ponta_Sem |

## 3. Facility Supervision and Monitoring of Water Supply

During the testing period the water supply did not present any problem related to interruptions or leakages. Initially, the water supply operated at a turbulent flow of $4.83 \times 10^{-4}$ m³/s and Reynolds (Re) equaling 32,257 (see Table 2). The water's input and output temperatures, Ti and To respectively, presented no significant differences during the measurements. Variations regarding temperature were observed solely when the reservoir water temperature was compared with the ambient temperature (Ta) (see Table 3). On the last week of testing, a reduction of 86% of the water flow occurred, resulting in a transition flow of $6.6 \times 10^{-5}$ m³/s and Re equaling 4,415 (see Table 2). This reduction was not enough to prevent the thermal exchanges with the PV module. The cause of the reduction can be attributed to the internal oxidation of the coil and sediment deposition caused by the increase of chlorine concentration on the reservoir water.

## 4. Control and Monitoring of the Cooling System

### 4.1. Control and Supervision

The daily period of electricity production, which was registered by the inverter during the 61 days of measurements, starts at 06:10 am and finishes at 07:00 pm on the longest day. The mean daily period of electricity production is 11 h:13 min, the maximum is 12 h:10 min (on the 05/03/2015) and the minimum is 10 h:10 min (on the 06/03/2015).

Table 2. Water flow measurements at the beginning and at the end of the testing period on the TF.

| Data | Unit | Beginning | End |
|---|---|---|---|
| Flow | $Q$ (m³/s) | $4.83 \times 10^{-4}$ | $6.6 \times 10^{-5}$ |
| Speed | $u$ (m/s) | 1.69 | 0.23 |
| Diameter | $D$ (m) | $1.91 \times 10^{-2}$ | $1.91 \times 10^{-2}$ |
| Kinematic Viscosity[a] | ν (m²/s) | $1.00 \times 10^{-6}$ | $1.00 \times 10^{-6}$ |
| Reynolds | Re | 32,257 | 4,415 |
| Flow type | - | Turbulent (Re > 10.000) | Transition (2.000 < Re < 10.000) |

[a]Kinematic Viscosity ($\nu(T, P)$) calculated in Normal Temperature and Pressure (NTP) Conditions.

Table 3. Input and output water temperatures (˚C) of the cooling system on the TF.

| Date (dd/mm/aaaa) | Time (hh:min) | $T_i$ (˚C) | $T_o$ (˚C) | $T_a$ (˚C) |
|---|---|---|---|---|
| 05/03/2015 | 10:09 | 21.0 | 21.0 | 28.9 |
| 16/03/2015 | 10:00 | 20.5 | 20.5 | 26.2 |
| 31/03/2015 | 10:00 | 21.0 | 21.0 | [(a)] |
| 14/04/2015 | 11:04 | 21.5 | 21.5 | 28.6 |
| 31/04/2015 | 10:29 | 20.5 | 20.5 | [(a)] |

[(a)]No ambient temperature available.

The analysis of the maximum and the minimum values, which occurred on consecutive days, reveals that climate factors have a strong influence on the production of electricity. This fact is more evident in Figure 4, if the days 16/04, 17/04 and 18/04 are analyzed, presenting practically the period of insulation, but different performance on energy output, 3.91 kWh/day, 6.69 kWh/day and 6.11 kWh/day, respectively, or in other words, the Relative Energy output per Daily Period of electricity (REDP) on each day varied by 8.46, 14.48 and 13.23, respectively. The maximum daily REDP registered during the testing period was equal to 16.34 and it occurred on the 27/03/2015, presenting a daily energy output of 7.70 kWh/day, which is lower than the energy output registered on the 02/04/2015 (7.82 kWh/day), with a lower REDP equaling 16.31 and a period of time equaling 11 h:25 min. If the lowest REDPs are analyzed, the minimum one (equals to 2.75) corresponded to the lowest energy output (1.31 kWh/day), registered on the 30/03/2015, although its period of electricity generation (11 h:24 min:47 s) was higher than the one registered on the day with the second lowest REDP (3.00)—occurred on the 22/04/2015 with energy output equaling 1.32 kWh/day and period equaling 10h: 5min. For the lowest period of electricity generation registered (10 h:10 min), the REDP was equal to 10.41 with energy output equaling 4.41 kWh/day (see Figure 4). The total energy output during the testing period was equal to 302.79 kWh, with a mean REDP equaling 10.61 and a mean daily energy output equaling 4.96 kWh/day.

### 4.2. Analysis of the Supervision and Control of the Performance of the Cooling Systems

An important analysis of energy systems is given through the energy Yield (Y), here meant as the ratio between net energy output and the systems installed capacity (kWh/kWp). The energy yield provides a relative measure that allows inter-comparison among different projects, dimensions, and technologies [8]. Another factor used for evaluating energy systems is so called capacity factor (CF), which correlates the net energy output and the theoretical energy output, both operating at the installed capacity during a 24 h per day.

Figure 5 presents the behaviour of both energy Yield (Y) and Capacity Factor (CF) during a period of eleven months. The variation is expected due to the season (dry or rainy), however the comparison between months 3 and 4, which

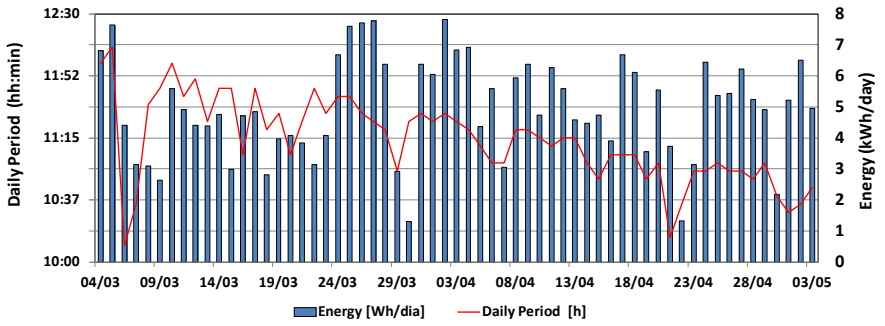


Figure 4. Daily period of electricity production (hh:min) and energy output (kWh/day).

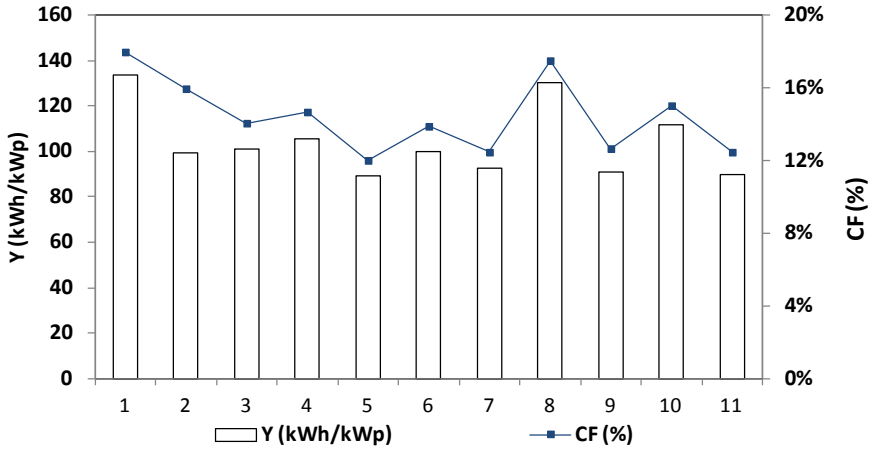


**Figure 5.** Monthly energy Yield (*Y*) and monthly Capacity Factor (*CF*).

correspond to the testing period, and the consecutive months (5, 6, 7, 8, 9, 10 and 11), reveal that these present a more oscillating behaviour. The overall energy yield is equal to 1659.97 kWh/kWp.

The analysis of the graphs on Figure 6 reveals that Y varies during the month and during the year. The maximum values of Y (Ymax) are less sensitive during the year, being higher than 4.94 kWh/kWp, whereas the minimum values of Y (Ymin) are more sensitive due to the influence of the season, presenting a more oscillating behaviour during the period between months 5 and 9 (dry season), presenting values lower than 1.0 kWh/kWp. In turn, the mean value of Y (Ymean) oscillates during the whole period, presenting values near the fourth quartile of the sample. During the testing period (month 4 and 5), the Ymin (0.90 and 0.91), and Ymean (3.4 and 3.5) present the lowest variations observed during the whole period, and the Ymax (5.36 and 5.39) presents the second lowest variation, indicating a better performance due to the application of the cooling system.

### 4.3. Temperature Monitoring of the Cooling System

The temperatures measured on the modules PV-2 (TPV-2), PV-3 (TPV-3) and PV-5 (TPV-5), with and without MCU, vary daily. By analyzing the data shown on Figure 7, it is possible to verify that the nocturnal temperatures registered on the PV modules without MCU are lower than the ones registered on the PV modules with MCU. This occurs because of the absence of solar radiation, mild ambient temperatures in comparison to the diurnal ones, and the thermal capacity of the circulating water, which is higher than the air's one, *i.e.* during the night the water losses less heat than the air, keeping the PV module's temperature higher than the ambient temperature. After starting the electricity production, the temperatures increase in both cases (with and without MCU). In the PV modules without the MCU this increase is more abrupt, reaching temperatures higher than the other modules in the beginning of the day, and remaining higher until the evening, if no other climatic event occurs, such as rainfall or long cloud cover emergence. The data measured on the 04/03/2015 shows a rela-

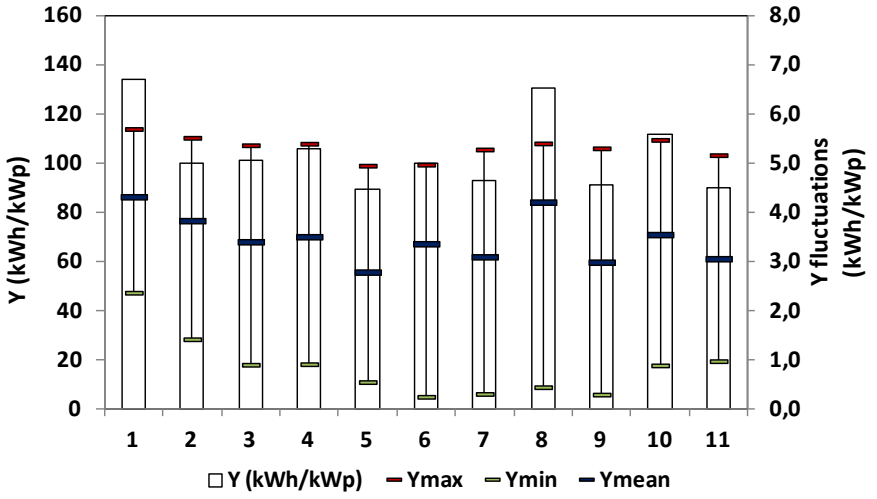


**Figure 6.** Monthly $Y$, $Y_{max}$, $Y_{min}$ and $Y_{mean}$ (kWh/kwp).

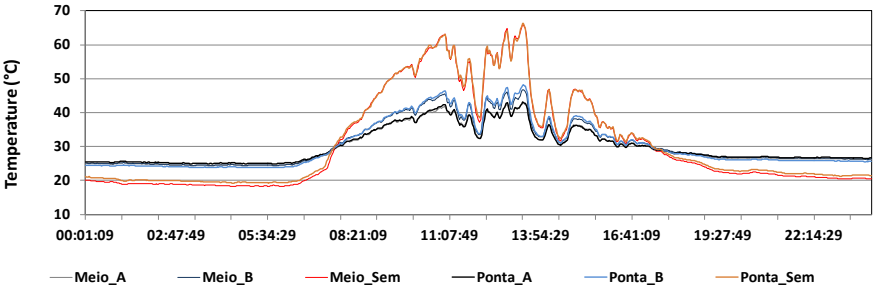


**Figure 7.** $T_{PV-2}$, $T_{PV-3}$ and $T_{PV-5}$ (°C) during 24h on 04/03/2015.

tively good performance for the period, presenting a REDP equaling 13.62 and an electricity output equaling 6.81 kWh/day—both above the mean value for the testing period.

On the 16/03/2015 the system presented a rather low performance since both the REDP (10.22) and the electricity output (4.72 kWh/day) lied below the average. By comparing the **Figure 8(a)** and **Figure 8(b)**, which show the electricity output and the operating temperature on PV-2, PV-3 and PV-5, it is possible to observe a correlation between both graphs in terms of the maximum and the minimum values. The electricity production presents a steady good performance until the early afternoon, with a peak of 410 Ws at 11:15:39 am, and declines right after 02:00:39 pm, reaching values lower than 30 Ws, which remained practically constant until the end of the day. The same can be observed for the temperatures (TPV-2, TPV-3 and TPV-5), which decreased because of the cloud cover and rainfall that directly affected the incident solar radiation and the ambient temperature.

Through the analysis of **Figure 9(a)** which shows TPV-2, TPV-3 and TPV-5 at 12:12:49 pm, it is possible to observe that the difference between the maximum temperature (Tmax = 68.06˚C) and the minimum one (Tmin = 42.45˚C) is 25.61˚C (see **Figure 9(b)**). These values registered on the 16/03/2015 were the highest values in terms of a maximum temperature and, therefore registered the

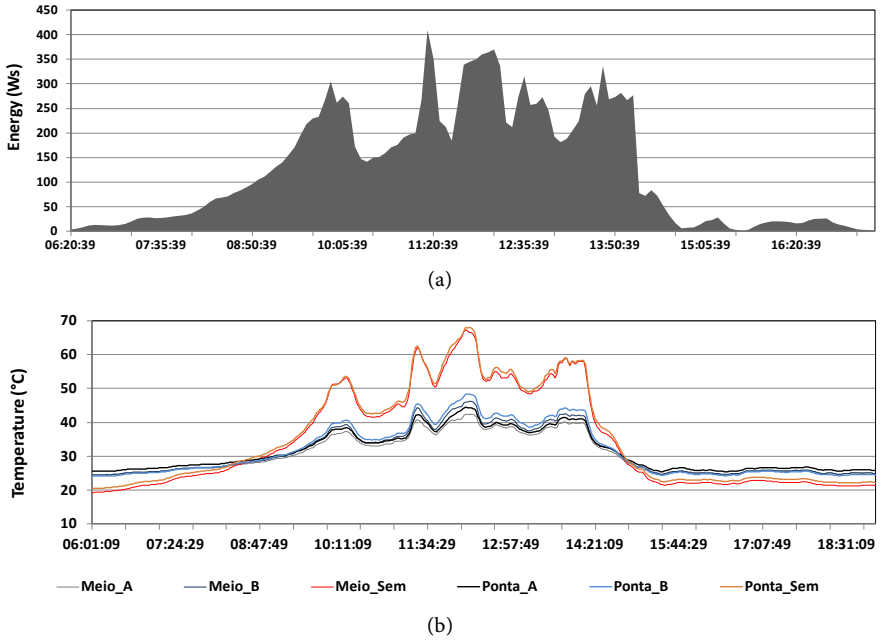


**Figure 8.** Performance of the TF on the 16/03/2015 (a) Electricity output (Ws) and (b) TPV-2, TPV-3 and TPV-5 (˚C).

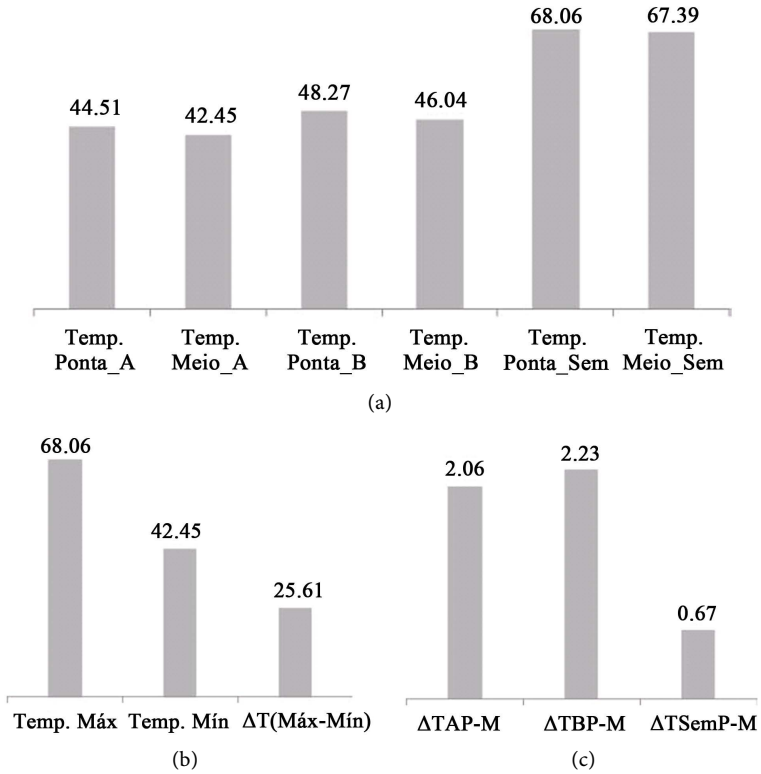


**Figure 9.** 16/03/2015, at 12:12:49 pm. (a) TPV-2, TPV-3 and TPV-5; (b) Tmax, Tmin and ΔT(max-min) and (c) ΔTPV.

highest difference among the minimum and the maximum temperatures during the testing period. By analyzing the temperature difference within the same PV module (ΔTPV), PV-3 presents ΔTPV-3 = 2.06˚C, PV-2 has ΔTPV-2 = 2.26˚C,

and PV-5 ΔTPV-5 = 0.67˚C. Furthermore, both temperatures registered on the PV-3 show that it operates below the Nominal Operating Cell Temperature (NOCT) de 47˚C ± 2˚C [3].

The highest electricity production occurred on the 02/04/2015, 7.82 kWh/day, presenting the second highest REDP equaling 16.31. **Figure 10** shows both the electricity output and the temperatures on the PV modules. In agreement with the previous results observed on the 16/03/2015, the graphs correlate with each other. The electricity production starts at 07:25 am, with a sharp increase until 10:35 am, reachin up to 300 Ws and keeping a steady electricity production of 300 Ws until 05:10 pm (apart from short periods of cloud covering), when the production starts declining, until the end of the operation at 06:55 pm. The peak of electricity production (407 Ws) was registered at 12:50 pm. The curve in the graph is similar to the ideal curve of electricity production of a PVPP [9], and solar irradiance [10] for a cloud-free day, presenting a sharp increase in the morning, steady production during the day, followed by an also sharp decrease until the end of day. The same behaviour was observed for the operating temperatures of the PV modules.

**Figure 11(a)** shows the temperatures (TPV-2, TPV-3 and TPV-5) on the 02/04/2015 at 12:52:23 pm, which registered Tmax = 57.31˚C on the sensor "Meio_Sem" of PV-5, whereas the minimum temperature was Tmin = 40.18˚C, registered on the sensor "Meio_A" of the module PV-3, resulting in a difference ΔT (max-min) =17.13˚C (see **Figure 11(b)**). If the temperatures on the same module are analyzed, it results ΔTPV-3 = 1.30˚C, ΔTPV-2 = 1.67˚C, and ΔTPV-5 = 2.65˚C (see **Figure 11(c)**). Furthermore, the temperatures registered on the PV-3 module show that it operates below the NOCT. Although the electricity

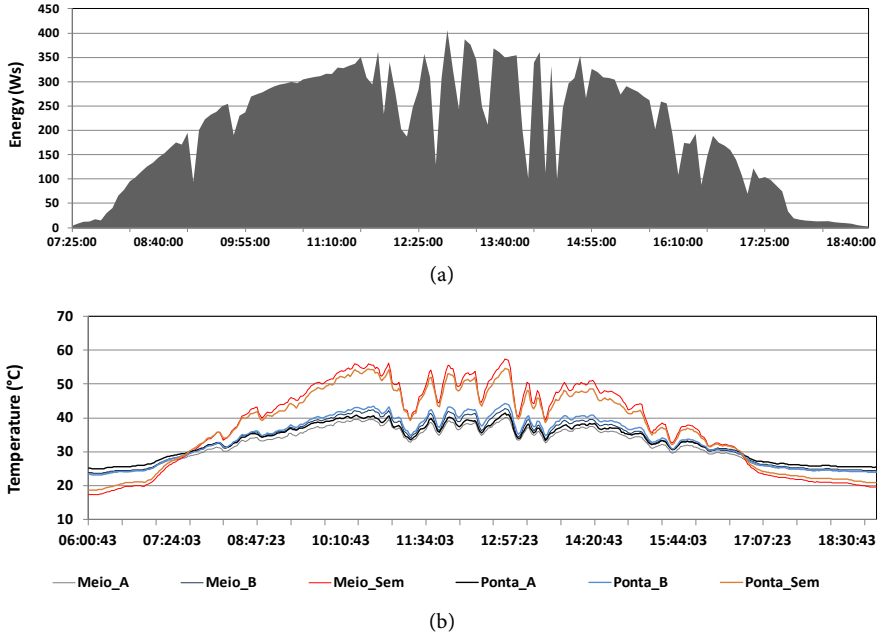


**Figure 10.** *TF* on the 02/04/2015. (a) electricity production ($W_s$) and (b) $T_{PV\text{-}2}$, $T_{PV\text{-}3}$ and $T_{PV\text{-}5}$ (˚C).

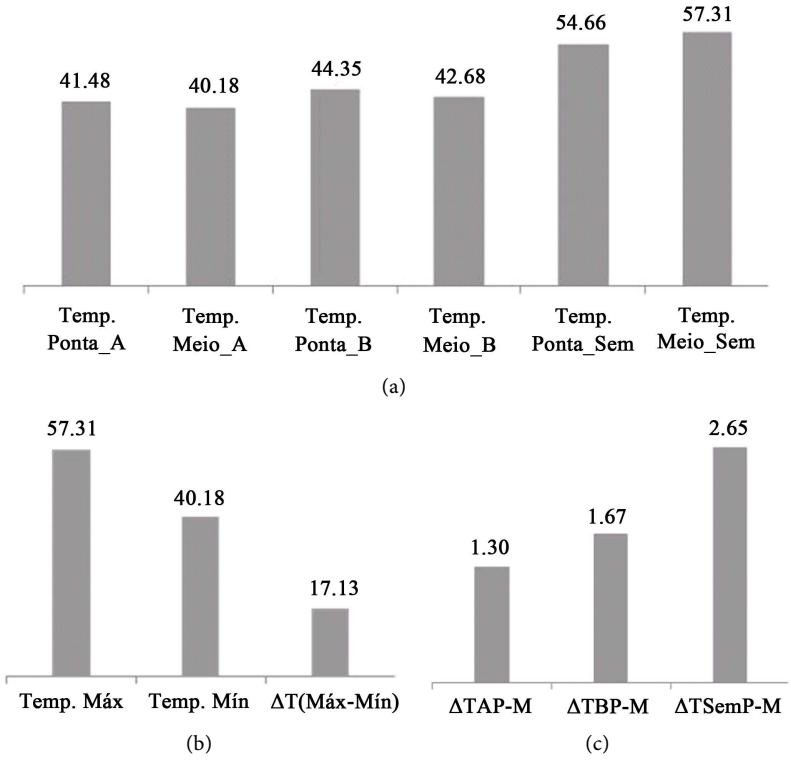


**Figure 11.** 02/04/2015, at 12:52:23 pm. (a) $T_{PV-2}$, $T_{PV-3}$ and $T_{PV-5}$; (b) $T_{max}$, $T_{min}$ and $\Delta T_{(max-min)}$ and (c) $\Delta T_{PV}$.

output shows the highest score for the testing period, the maximum temperature registered on this day was 10.75˚C lower than the one registered on the 16/03/2015. Moreover, the Tmax registered on the 02/04/2015 occurred at the sensor "Meio_sem", whereas the one registered on the 16/03/2015 occurred on the sensor "Ponta_Sem".

During the testing period, 235 measurements of temperature were higher than 60˚C and they were observed on 21 days, representing 34.4% of the period. These measurements presented a mean value (Tmean) equaling 62.01˚C, the minimum equaling 60.01˚C, and the maximum equaling 68.06˚C. The observations occurred exclusively on the PV-5 module, from which 77.0% occurred on the sensor "Meio_Sem". At the same time, the minimum temperatures were registered on the PV-3 module, from which 97.4% occurred in the sensor "Meio_A" (see **Figure 12(a)**), with a mean temperature equaling 41.48˚C, a minimum temperature equaling 39.4˚C, and a maximum one equaling 43.55˚C. The mean temperature difference between the sensors was 20.53˚C, with a minimum equaling 17.79˚C, and a maximum equaling 25.61˚C.

In terms of the temperature difference among the same PV module (see **Figure 12(b)**), PV-3 presented a mean value of 1.13˚C (the lowest mean value among the modules), a minimum value equaling 0.01˚C, and maximum equaling 3.68˚C; PV-2 presented an average temperature difference equaling 1.69˚C, with a minimum of 0.63˚C, and a maximum equaling 2.34˚C; PV-5 presented an average value equaling 1.43˚C, a minimum value equaling 0.01˚C, and a maximum

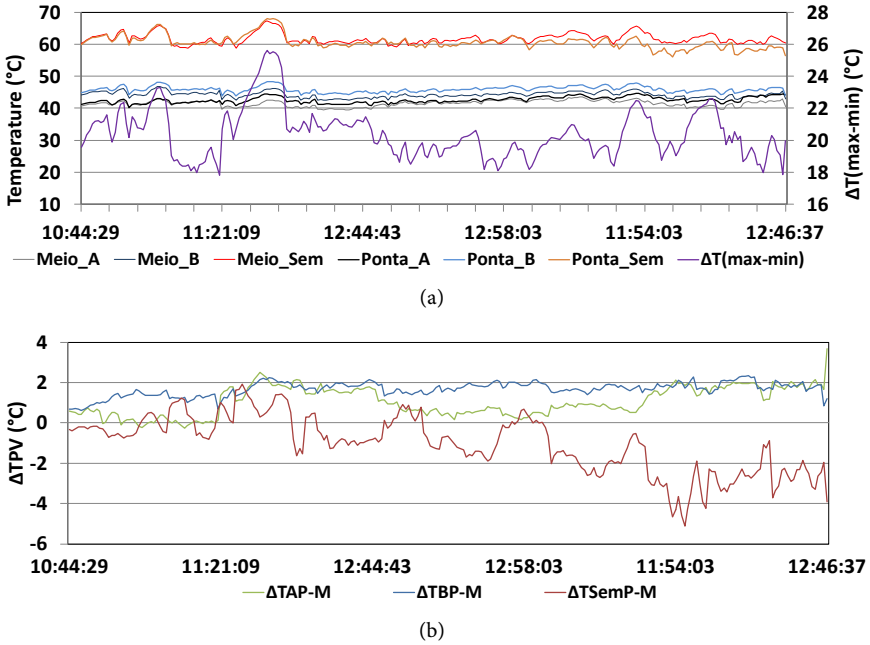


**Figure 12.** $T_{PV} > 60$ ˚C. (a) $T_{PV-2}$, $T_{PV-3}$, $T_{PV-5}$ and $\Delta T_{(max-min)}$; (b) $\Delta T_{PV}$.

equaling 5.12˚C (the highest maximum value observed). Moreover, the temperatures registered on the PV-3 module show that it operated once more below the NOCT, with maximum temperatures equaling 43.55˚C and 44.75˚C, respectively on the sensors "Meio_A" and "Ponta_A" (see Table 4).

## 5. Cooling System of the *TF*

Several photos were taken on the 04/03/2015 at three different times (10:00 am, 12:00 pm and 03:00 pm). The focus was to cover the region where the sensors PT-100 were applied on the inferior surfaces, and the superior surfaces of the PV modules.

The analysis of the images revealed the temperatures ordered as TPV-3 < TPV-2 < TPV-5, corroborating the observations obtained from the sensor PT100 (see Table 5). The highest temperature (56.6˚C) was registered at 10:00 am on the sensor "Meio_Sem" in the PV-5 module. Except for the PV-3 module, the highest temperatures were registered in the region where the sensor SM is applied. Still, both the PV-3 and the PV-5 modules registered the highest temperatures at 10:00 am, whereas the PV-2 module presented the highest temperature at 12:00 pm. The lowest temperatures were registered at 03:00 pm in all the modules; with the lowest value equaling 32.3˚C observed in the region of the sensor "Meio_A" of the PV-3 module, followed by the PV-2, with a value equaling 35.5˚C in the region of the sensor "Ponta_B", and then the PV-5 module, with a value equaling 43.7˚C in the region of the sensor "Ponta_Sem". Regarding the temperature on the superior surface of the modules, the PV-1 presents the highest temperatures for all the periods of observation. In terms of distribution across the surface, the PV-1 module presented a more uniform distribution (see Figure 13). The place with the highest temperature in the PV-1 module is the

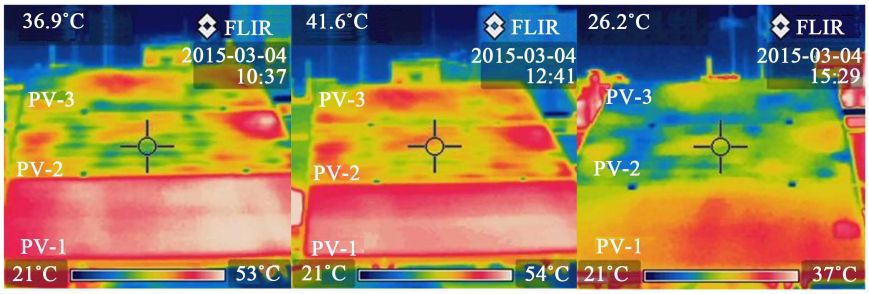


(a) (b) (c)

**Figure 13.** Superior surface of the *PV* modules. (a) 10:00 am; (b) 12:00 pm and (c) 03:00 pm.

**Table 4.** $T_{mean}$, $T_{min}$ and $T_{max}$ with $T_{PV} > 60^{\circ}C$.

| PV | Cooling Model | Sensor PT-100 | $T_{mean}$ (˚C) | $T_{min}$ (˚C) | $T_{max}$ (˚C) |
|---|---|---|---|---|---|
| 2 | Model B | Meio_B | 44.21 | 42.49 | 46.76 |
| | | Ponta_B | 45.90 | 43.84 | 48.33 |
| 3 | Model A | Meio_A | 41.48 | 39.40 | 43.55 |
| | | Ponta_A | 42.61 | 40.24 | 44.75 |
| 5 | - | Meio_Sem | 61.86 | 58.86 | 67.39 |
| | | Ponta_Sem | 60.73 | 56.06 | 68.06 |

**Table 5.** Results from thermographic camera.

| Period (hh:min) | PV | Cooling Model | Sensor PT-100 | T (˚C) |
|---|---|---|---|---|
| 10:00 am | 2 | Model B | Meio_B | 40.9 |
| | | | Ponta_B | 39.2 |
| | 3 | Model A | Meio_A | 36.6 |
| | | | Ponta_A | 37.1 |
| | 5 | - | Meio_Sem | 56.6 |
| | | | Ponta_Sem | 55.4 |
| 12:00 pm | 2 | Model B | Meio_B | 41.9 |
| | | | Ponta_B | 40.0 |
| | 3 | Model A | Meio_A | 36.1 |
| | | | Ponta_A | 35.5 |
| | 5 | - | Meio_Sem | 55.2 |
| | | | Ponta_Sem | 54.0 |
| 03:00 pm | 2 | Model B | Meio_B | 35.7 |
| | | | Ponta_B | 35.3 |
| | 3 | Model A | Meio_A | 32.3 |
| | | | Ponta_A | 33.5 |
| | 5 | - | Meio_Sem | 44.1 |
| | | | Ponta_Sem | 43.7 |

region near the junction box, specifically the lower right corner, where the energy transmission takes place.

## 6. Conclusions

The supervision and monitoring of the PV modules (as the models A and B) were not trivial tasks, since the technology is new, lacking a solid theoretical background, and challenging the interpretation of its real operation. In order to overcome such limitations, the previous elaboration of the methodology produced satisfactory results.

The water supply system operated permanently and without leakages to the ducts and junctions. The operation of the system had no influence on the amount of water stored in the reservoirs. The temperature of the water at the entrance and at the exit remained equal. The only issue regarding the water supply system was the difference in the water flow if compared to the beginning and the end of the testing period, varying by 86%.

The results show that the PV-2 and the PV-3, both with a cooling system, operated at lower temperatures than the PV-5, without a cooling system. The daily maximum temperatures occurred exclusively in the *PV*-5 module, with $T_{\text{mean}}$, $T_{\text{mín}}$ and $T_{\text{max}}$ equaling 62.01˚C, 60.01˚C and 68.06˚C, respectively. The difference between these temperatures and the minimum ones is 20.53˚C higher than the average, with a minimum difference equaling 17.7˚C, and a maximum equaling 25.61˚C. All minimum temperatures were registered on the sensor PT-100 in the *PV*-3 with cooling system model A.

The comparison between PV-2 and PV-3 reveals that PV-3 always operates at temperatures below 45˚C. Thus, the cooling system model A allows the the PV modules to operate at a temperature below the NOCT, since the maximum temperatures observed in the PV-3 were 43.55˚C and 44.75˚C, in the sensors Meio_A and Ponta_A, respectively. Moreover, the differences between the temperatures registered in the same module are lower in the PV module with the cooling system model A (the average value equaling 1.13˚C), than the ones registered in the PV module with the cooling system model B (the average value equaling 1.69˚C).

The analysis of the performance factors (Y and FC) indicates that the TF presented lower monthly oscillations when the cooling system operates (Ymin and Ymean 0.01 and 0.1, respectively).

Therefore, the model of MCU selected for a large-scale application that is to be installed as the prototype of the PVPP is the model A.

## Acknowledgements

To CAPES, for the scholarship, to CESP for funding the R & D ANEEL PE-0061-0037/2012 which enabled the conclusion of this article. To the team of GEPEA/EPUSP researchers and collaborators who helped direct and indirectly on the accomplishment of this R & D project.

## References


[1] de Souza Martins, H.H.T. (2004) Metodologia qualitativa de pesquisa. *Educação e Pesquisa*, **30**, 289-300. https://doi.org/10.1590/S1517-97022004000200007

[2] ANEEL (2013) Desenvolvimento de Equipamento de Usina Solar Fotovoltaica com Sistema Ativo de Arrefecimento para maior Rendimento na Geração de Eletricidade. Projeto Estratégico de Pesquisa e Desenvolvimento, ANEEL PE-0061-0037.

[3] SunEdison (2012) MEMC Silvantis™ P290 Modulo. Data Sheet_Q2 2012. SunEdison, Maryland Heights, St. Louis County, Missouri,

[4] KSB (2007) KSB Hydrobloc P500 monofásica 220V: Data Sheet No. A2748/49.8P/6. KSB, Frankenthal.

[5] Novus (2014) Termorresistências Pt100. http://www.novus.com.br/downloads/Arquivos/folheto_pt100.pdf

[6] Novus (2015) Manual de Instruções Field Logger.

[7] Flir (2010) Termovisores Compactos: Características dos Termovisores FLIR i5 eFLIR i7. Flir Systems, Wilsonville.

[8] Marion, B., Adelstein, J., Boyle, K., Hayden, H., Hammond, B., Fletcher, T., Canada, B., Narang, D., Shugar, D., Wenger, H., Kimber, A., Mitchell, L., Rich, G. and Townsend, T. (2015) Performance Parameters for Grid-Connected PV Systems. *Proceedings of the* 31*st IEEE Photovoltaic Specialists Conference and Exhibition*, Lake Buena Vista, 3-7 January 2005, Article ID: 8478977.

[9] Silva, V.O., Veiga Gimenes, A.L.V., Ribeiro Galvão, L.C. and Morales Udaeta, M.E. (2015) Study, Verification and Selection of Cooling System Model for PV Modules with Verification Prototype. *Proceedings of the EU PVSEC*, Hamburg, 14-18 September 2015, 2153-2158.

[10] Junior, H. de S.M., Cavalcante, R.L., Galhardo, M.A.B. and Macedo, W.N. (2012) Aplicação de Energia Solar Fotovoltaica—Um estudo de Caso na Região Amazônica. *Revista Geonorte*, **2**, 1303-1309.